SAND2024-05589J

Control of quantized spontaneous emission from single GaAs quantum dots embedded in Huygens' metasurfaces

Prasad P Iyer[1,2*], Samuel Prescott[3], Sadhvikas Addamane[1,2], Hyunseung Jung[1,2], Jacob Henshaw[1,2], Andrew Mounce[1,2], Ting S Luk[1,2], Oleg Mitrofanov[3], Igal Brener[1,2*]

1. Center for Integrated Nanotechnologies, Sandia National Lab, Albuquerque NM, USA, 2. Sandia National Laboratories, Albuquerque NM, USA 3. University College London, Electronic and Electrical Engineering, London WC1E 7JE, UK

*ppadma@sandia.gov, ibrener@sandia.gov

Abstract: Advancements in the field of photonic quantum information systems (QIS) have driven the development of high-brightness, on-demand, highly indistinguishable semiconductor epitaxial quantum dots (QDs) as single photon sources. Strain-free, monodisperse, and spatially sparse local-droplet-etched (LDE) epitaxial semiconductor QDs have recently been demonstrated as a superior alternative to the traditional Stranski-Krastanov QDs. However, integration of these LDE QDs into resonant nanophotonic architectures with the ability to scale to many and interacting QDs is yet to be demonstrated. In this letter, we present a potential solution realized by embedding isolated LDE QDs within a Huygens' metasurface formed using the spectral overlap of the fundamental electric and magnetic dipolar resonances. We demonstrate for the first time a position- and size-independent one order of magnitude increase in the collection efficiency and emission lifetime control for single-photon emission from LDE GaAs QDs embedded within resonant semiconductor ($Al_{0.4}Ga_{0.6}As$) Huygens' metasurfaces. Our results represent a significant step towards leveraging the advantages LDE QDs within a nanophotonic architecture to meet the scalability demands of photonic QIS.

Introduction

Research into on-demand, single and entangled photon sources for all areas of quantum information processing has been actively pursued for the past several decades. The development of these sources has evolved in parallel using parametric processes [SPDC refs, our Science], and a variety of single photon emitters coupled to engineered photonic structures [some review]. For the latter type, epitaxial quantum dots (QDs) offer clear advantages, such as wavelength tunable emission, on demand operation, high brightness, high degree of indistinguishability, versatility in entangling photons to other degrees of freedom such as spin, and finally, monolithic integration with photonic cavities or other photonic circuits. Among epitaxial QD, local-droplet-etched (LDE) epitaxy QDs are particularly attractive as they form a deeper confinement potential compared to Stranski-Krastanov (S-K) QDs, offer a greater freedom in choosing the dot and host material composition and their areal density, providing a path to wider emission tunability and integration [many refs here].

Alongside improvements in QD epitaxy, we can now leverage recent advancements in nanophotonics to enhance photon collection efficiency, control the angular momentum, entangle different degrees of freedom and manipulate interactions between a finite-number of quantum emitters. However, the integration of QDs into resonant nanophotonic cavities, which can couple these QDs, is very challenging due to requirements on sub-nm scale accurate placement and on precise control of the emission wavelength with respect to the cavity resonances. These requirements are critical for scaling up QD sources for quantum information systems (QIS). To overcome the QD limitations, specifically, their random location and size (which defines the emission wavelength) researchers have attempted epitaxial QD growth in nanofabricated etch-pits [ref] and fabrication of nanophotonic cavities after determining the location of QDs. However, these approaches have limited scalability for multiple QDs and so far have resulted in low-brightness emitters [ref]. Here, we demonstrate that semiconductor metasurfaces with embedded LDE QDs can form a potential solution to overcome the randomness of QD localization inherent to the epitaxial growth process while taking advantage of the greater monodispersity, brightness and sparsity of these QDs [ref]. The metasurfaces offers an attractive platform where a single design can enhance the emission properties of all the LDE QDs grown on the wafer regardless of their size and position. Furthermore, the monolithic integration of LDE QDs into the metasurface offer a robust semiconductor platform for scientific exploration and future applications. We demonstrate that $Al_{0.4}Ga_{0.6}As$ Huygens' metasurfaces provide an average of 10x enhancement of the collected photoluminescence (PL) from the embedded single LDE QDs when compared with QDs in an unpatterned region. The enhanced efficiency enables single-photon spectroscopy of excitonic species in LDE QDs with excitation power densities over an order of magnitude lower than the same QDs present in unpatterned thin films. Surprisingly, we discovered that at the low CW-

pump power densities incident on the metasurface (< 10W/cm^2, 515nm), the effective lifetime of single photon emitters can be dynamically controlled by nearly an order of magnitude (8ns – 1ns) with the pump power. Ultimately, a metasurface with embedded high brightness LDE QDs could provide an efficient route towards realizing scalable-coupled quantum meta-atoms suitable for quantum information processing, sensing and communications.

Results and Discussion

A Huygens' metasurface forms an ideal platform for embedding isolated semiconductor QDs because of spatial uniformity of modes within individual resonators, created by overlapping the fundamental electric and magnetic dipolar (ED and MD) resonances [ref]. This spatial uniformity of the resonant fields (Fig 1a) minimizes the effect of random positioning the QD within the resonator. Additionally, the broadband spectral response of the overlapping dipolar resonances covers the wavelength distribution of QD emitters grown on the wafer. $Al_{0.4}Ga_{0.6}As$ is a suitable host for GaAs LDE QDs because of the larger bandgap (E_g ~ 2.039eV or 607.8nm at 15K [ref]) and high refractive index (n = 3.43 [ref]) required to form resonant semiconductor metasurfaces. The modal dispersion of the fundamental electric and magnetic dipolar modes can be engineered by controlling the geometry (width, sub-wavelength pitch and height) of the $Al_{0.4}Ga_{0.6}As$ resonators.

$Al_{0.4}Ga_{0.6}As$ thin films with embedded GaAs LDE QDs were epitaxially grown (see Methods) and fabricated into metasurface resonators. We used a flip-chip process (see Methods) to eliminate the influence of the high index absorbing GaAs substrate on embedded QD emitters (Fig. 1b) []. In this process, we leverage the precise control of the QDs' vertical positioning within the resonators provided by the epitaxial growth.

Figure 1c shows that the PL peak intensity (measured at 15±5K) from an isolated GaAs LDE QD embedded within an exemplar Huygens' metasurface is enhanced by an order of magnitude when compared to the QD emission from an unpatterned slab. Furthermore, the PL image (inset in Fig, 1c) demonstrates that the emission enhancement from the QDs (surviving the nanofabrication process) is agnostic of the position of the QDs within the metasurface. Interestingly, the distribution of emission wavelength for the QDs present on the wafer (both within the metasurface and the unpatterned region) overlaps well with the spectral band where the metasurface supports the fundamental electric and magnetic dipolar resonances (see SI). The band, centered at 745 nm, manifests itself as a local maximum in the metasurface transmission spectrum (Fig. 1d). This spectral overlap specifically highlights the capability of the low-Q modes to enhance QD emission regardless of the size distribution gained during the LDE growth process. The position- and emission wavelength-agnostic enhancement of isolated embedded LDE GaAs QDs show the

potential for Huygens' metasurfaces not only as a characterization platform of novel QDs but also as a platform to engineer the interactions between isolated QDs through resonant near-field interactions.

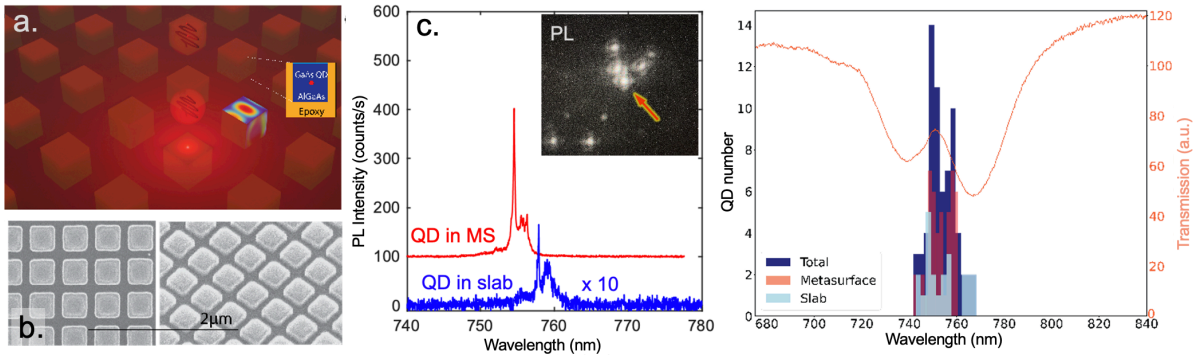

Figure 1. Photoluminescence enhancement with Mie metasurfaces. a. Illustration of Huygens' metasurface (MS) made of AlGaAs resonators with an embedded GaAs quantum dot (QD). The color-maps on the resonators' top and side surfaces show the normalized electric field profiles (min – blue, max – red) of optical resonances. **b.** Scanning electron microscopy (SEM) images of fabricated metasurfaces with a top (left) and tilted (right) views. These images were taken prior to the flip-chip bonding step. **c.** Photoluminescence (PL) spectra of GaAs LDE QDs from a Huygens' metasurface and from a uniform epitaxial layer (slab) demonstrating an order of magnitude increase of PL emission into free space. The inset shows a microscope PL image where individual QDs within the metasurface cane be seen. **d.** Distribution of QD exciton (X) emission wavelength for 80 randomly selected LDE GaAs QDs within the metasurface (red), the slab (light blue) and the total (dark blue). The center of this narrow distribution (< ±5nm) is aligned with the Huygens' point for selected metasurface, identified as a local peak at 750 nm in the metasurface transmission spectrum (orange curve).

To evaluate the effect of the metasurface modes on the PL, we collected spectra of several QDs embedded into three metasurfaces of different designs (Fig. 2a-c) and compared them to PL from QDs embedded in a uniform layer of $Al_{0.4}Ga_{0.6}As$ (referred here as the slab) (see Methods for details). Figures 2d-f summarize the peak PL intensity and the central wavelength of emission for the tested single QDs. For MS1 and MS3 with the ED and MD modes overlapping with the wavelength of QD emission (Fig. 2a,c), the average PL intensity is higher by a factor of ~10 in comparison to the average emission from QDs embedded in the slab (Fig. 2d,f). In contrast, MS2 with the ED and MD modes at ~825 nm (Fig. 2b), outside the region of QD PL emission, show only marginal enhancement (~2) (Fig. 2e). From these results and assuming that the photonic environment does not affect the emission rate appreciably (see SI), we conclude that the ED and MD modes aligned with the QD emission wavelength yield a one order of magnitude increase in the number of outcoupled photons. Furthermore, our metasurface fabrication process does not deteriorate the QD emission properties.

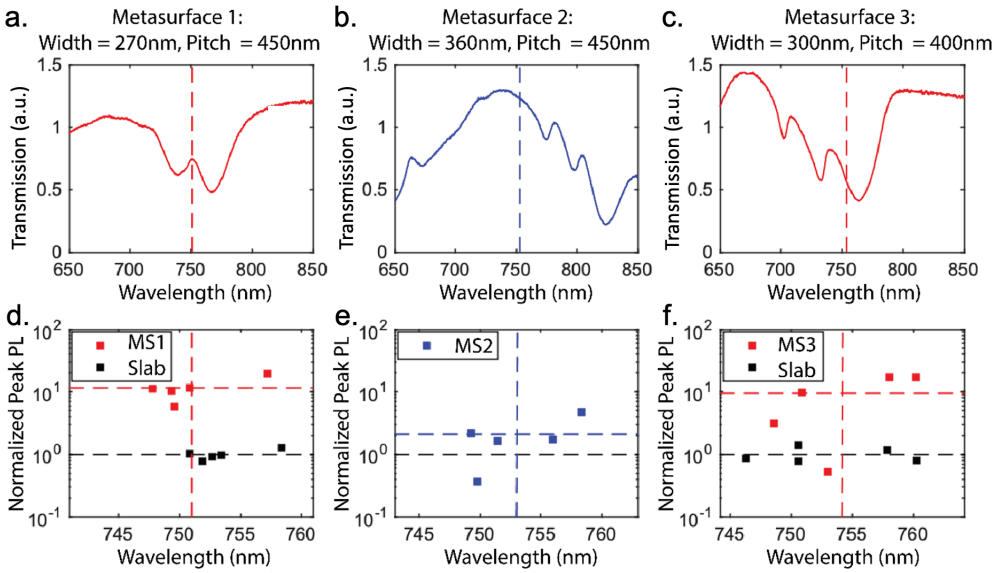

Figure 2. Metasurface optical properties and corresponding QD PL emission enhancement. a-c. Transmission spectra of three metasurfaces (MS) of different geometry (resonator width and pitch). The spectra are normalized to transmission through the substrate. The Mie modes are aligned with the QD emission wavelength for MS1 and MS3, and red-shifted by more than 50 nm for MS2. **d-e.** PL peak intensity for the dominant exciton transition from 5 randomly selected QDs within MS1, MS2 and MS3, and form QDs located in the unpatterned slab. PL intensity for every QD is normalized to the average peak intensity of QD PL from the slab. Dashed lines mark the average values for each MS.

To reveal the underlying mechanisms that lead to the observed enhancement of photon emission we evaluated the effect of the metasurface on coupling the emission from QDs into free space using numerical electromagnetic simulations. We modelled a QD emitter as a point source of electromagnetic radiation placed inside the metasurfaces. It is important to note that due to a relatively low density of QDs (~0.1 μm^{-2}), we can assume that a Mie resonator with a dot is surrounded by resonators without dots. Therefore, the commonly used periodic boundary conditions [Ref] do not represent a realistic system. Thus, we chose to model a larger area metasurface. Furthermore, the lateral position of the QD within the resonator and the orientation of the QD dipole moment are both random. To evaluate a realistic effect of the metasurface on the QD emission we positioned a Mie resonator with a point source emitter in the center of a 9x9 array of passive resonators (as illustrated in Fig. 3a). We then simulated the light emission from the point source positioned in 9 different locations within the central resonator (Fig. 3b) and with three primary orientations of the dipole moment (x, y and z). The full set of positions and dipole moment orientations represents 27 equally probable cases of single QDs embedded in the Mie resonator (assuming that all the dipole orientations are equally probable; see SI for simulation details). To quantify the metasurface effect we compared the QD emission spectrum for the metasurface (averaged over the 27 cases)

to that for a $Al_{0.4}Ga_{0.6}As$ slab with embedded QDs. A normalized spectrum of QD emission from the metasurface is shown in Fig. 3c. The emission enhancement factor has a peak value of ~25 at exactly the wavelength where the ED and MD modes overlap (~750 nm, Fig. 3d,e). We note that the simulations show enhancement for emission both into the air and into the sapphire substrate. However, for this metasurface design and at this wavelength, the enhancement factor for emission into air is higher in comparison to the emission into the substrate (a factor of ~16).

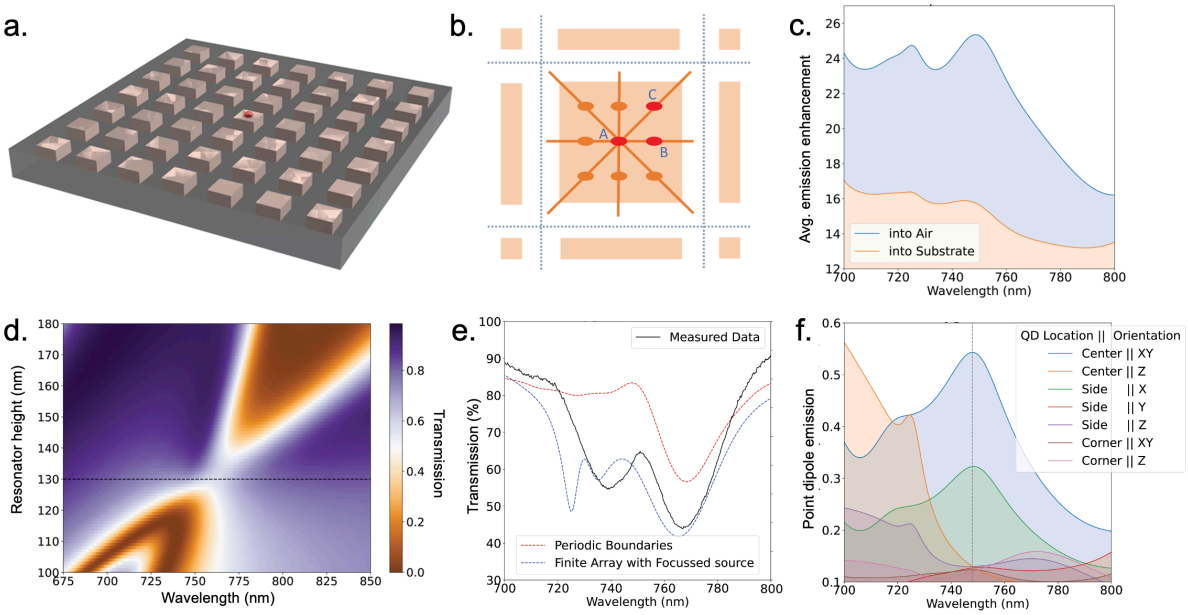

Figure 3: Full wave simulation of emission from Mie metasurfaces. a. Illustration of a finite array (7x7) of resonators with a QD in the central resonator used in the FDTD simulations. **b.** Schematic representing 9 simulated positions of the QD within the resonator. Red dots show the three unique locations (Center – A, Side – B and Corner – C). **c.** Average emission enhancement for a point dipole embedded within the metasurface resonator (blue- into air and orange – into substrate) with respect to the same source embedded into an unpatterned slab. **d.** Metasurface transmission map showing the dispersion of the electric (ED) and magnetic (MD) dipolar modes for a varying resonator height. The ED and MD modes overlap to form the Huygens' metasurface for h = 130 nm (marked by the horizontal dashed line) at a height of 130nm. **e.** Full wave simulation of the transmission spectrum (dashed blue line) and the experimentally measured transmission spectrum of the Huygens' metasurface (black line) using weakly focused (NA = 0.15) incident light. A simulated spectrum for periodic boundary conditions is shown by the red line for comparison. **f.** Emission spectra of the point dipole source placed at positions A, B and C with different dipole moment orientations (x,y – in plane and z – out of plane). Emission efficiency peaks at ~750 nm for the QD placed at the center (blue line) and at the side (green) locations for the *x*-oriented dipole.

The spectrum in Fig. 3c shows that the QD emission is enhanced not only at ~750 nm but within a wide band with a complex spectral structure. The source of this structure is revealed in Fig. 3f by plotting enhancement spectra for individual dipole moment orientations and QD positions within the resonator. This decomposition of the overall enhancement allowed us to correlate the main enhancement peak with specific locations and dipole orientations of the point emitter. The main peak at 750 nm is undoubtedly caused by the ED mode coupled to a QD positioned at the center of the resonator with the dipole moment in the

metasurface plane (point A in Fig 3b). A QD shifted half-way to the side (point B) also shows a main peak at 750 nm, albeit with reduced enhancement. These two positions/orientations are expected to couple most efficiently to the ED mode due to the spatial overlap with the ED mode profile. We therefore conclude that the observed emission enhancement at 750 nm can be assigned primarily to the spatial and spectral overlap of the ED mode with the QD emission. Other modes, including the MD mode, which is expected to be excited most efficiently by a QD positioned at Point C and having the dipole moment along the z-axis, also contribute to the overall enhancement, however at a lower level (less than 20% relative to ED).

To evaluate the potential of QDs embedded in the Huygens' metasurfaces as single-photon sources, we analyzed single-photon emission from isolated QDs and its dependence on optical pump intensity for non-resonant continuous wave (CW) excitation at 515nm. First, we characterized the PL saturation characteristics of a representative QD within the metasurface by measuring the PL spectrum dependence on the pump intensity. At low intensities (< 100W/cm^2), we observed a narrow (resolution-limited) QD spectrum, which broadens as the pump power is increased. Spectrum broadening has been observed previously in QDs at high intensities of excitation, and it has been attributed to carrier accumulation near the dot under excitation [ref]. In addition to the broadening, we observed that the photon emission rate for the dominant QD transition (at 761nm) started saturating above ~180W/cm^2 of excitation intensity. A similar saturation behavior occurred for a representative QD within the slab albeit at a slightly higher intensity (~280W/cm^2) (see SI). We then performed second order auto-correlation statistics measurements ($g^2(t)$) in the low excitation intensity regime using a Hanbury-Brown-Twiss (HBT) interferometer (see Methods). We measured $g^2(0)$ ~ 0.2-0.3 for a pumping power of ~10W/cm^2 (Fig 4b). We note that this result is achieved without the use of narrow (sub-GHz) spectral filters.

The $g^2(t)$ traces (Fig. 4b) show that the QD excitation lifetime increases at low pumping powers. For quantitative analysis, the measured $g^2(t)$ traces at each pump power were fitted using the equation $g^2(t) = 1 - ae^{-\frac{|t|}{\tau}}$, following the procedure in ref [2001 PRB]. Here *a* represents the purity of the single photon source such that $a = 1 - g^2(t=0)$ and τ represents the lifetime of the QD. We discovered that the effective lifetime of the single-photon emission from LDE QDs varies by nearly an order of magnitude: under very low excitation intensity (10W/cm^2), we observed a lifetime of 6.0 ±1 ns. It decreases by almost an order of magnitude (1.0±0.34ns) as we increased the intensity to 85W/cm^2 (Fig 4c). By tracking the photon emission rate (1/τ) as a function of the optical pump power we found a linear trend which when extrapolated to zero yielded an intrinsic lifetime of the QD-metasurface system of 8.73±1.2ns (Fig 4c).

This intrinsic lifetime for the GaAs LDE QDs-metasurface system (while operating as a single photon source) is surprising. First of all, the intrinsic lifetime of GaAs LDE QDs has been previously

estimated to be less than 400ps [Ref]. Secondly, nano-patterning of light-emitters typically reduces the effective lifetime due to the increase of surface-related defect states [Ref]. In contrast, here, both dots embedded in the metasurface and in the slab (see SI) show longer lifetimes than previously reported in the literature. This indicates that the metasurface fabrication process – including the nanoscale dry etching – has not degraded the QD emission properties.

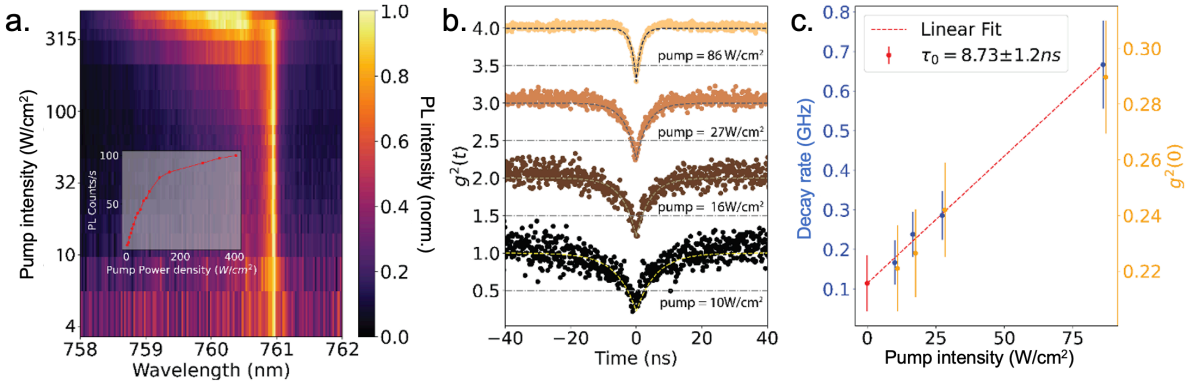

Figure 4. Single-photon characteristics of an isolated QD. a. Map of PL spectra from a single QD within the metasurface under continuous wave (CW) pumping at 515nm (spectra are normalized for each pump power). The CW pump power increases along the vertical axis (log-scale). The bright streak at 760.9 nm represents the X transition of the QD which undergoes spectral broadening under high pump powers. Inset: Peak PL intensity as a function of the pump power. The QD emission exhibits saturation after 100W/cm^2 of focused illumination. **b.** Waterfall style plot of the photon auto-correlation function from the same single QD under varying pump powers (10W/cm^2 – 86W/cm^2). The dashed lines represent the single exponential fits to the rising edge of the $g^2(t)$ plots. **c.** QD decay rate (left axis, blue dots) as a function of the pump power. The rate values are extracted from fitting the $g^2(t)$ traces in **b.** (dashed lines). The red dashed line represents a linear fit to the blue dots. Extrapolation of the linear fit to zero pump power gives an intrinsic QD exciton lifetime of 8.73±1.2ns (red dot). The anti-bunching dip at $t = 0$ is plotted in orange on the right axis to demonstrate that the QD behaves like a single-photon source under these pump powers.

In previous demonstrations of controlling the emission lifetime of a single QD (for example performed with an InAs SK QD coupled with a micro-disk cavity) a large difference in the lifetime between the QDs in the cavity and in an unpatterned region was attributed (tentatively) to Purcell suppression [ref]. However, FDTD simulations (matching experimental spectra) indicate that the Purcell factor for emitters embedded into the Mie resonator is close to 1 (see SI), suggesting that we are not extending the lifetime through Purcell suppression of emission. Furthermore, the lifetime estimates derived from the $g^2(t)$ measurements give an effective performance of the QD-metasurface system which cannot be attributed solely to the intrinsic lifetime of the GaAs QDs. The pump excites charge carriers in both the GaAs QD and in the $Al_{0.4}Ga_{0.6}As$ resonator. Hence, the effective lifetime of the QD emission results from two pathways – namely, direct excitation of the carriers in the QD and capture of carriers excited in the AlGaAs resonator. Additional experiments varying the optical pump wavelength from 515 nm to the emission

wavelength at 761nm need to be performed to separate these two excitation pathways. Ultimately, we have identified that the effective lifetime of the embedded QD can be varied by an order of magnitude by varying the optical pump power.

In conclusion, we have demonstrated an order of magnitude enhancement in emission intensity for LDE GaAs QDs embedded within a Huygens' metasurface independent of the QD placement with respect to the Mie resonator and the QD emission wavelength. We have developed a combination of novel monolithic QD growth, nanophotonic design and nanofabrication, which enabled us to collect the emission from an isolated QD embedded within the metasurface. We have demonstrated that overlapping the fundamental dipolar Mie modes with the emission wavelength of the QDs results in the observed enhancement, with the electric dipolar mode providing the main contribution while the Purcell factor remains close to 1. These realizations enabled us to control the lifetime of the metasurface-embedded QDs by an order of magnitude by varying the optical pump power. The monolithic semiconductor architecture demonstrated here could offer an ideal platform for characterization and calibration of the embedded LDE QDs whose emission could be tuned through the epitaxial growth and enhanced by the Huygens's metasurface geometry over the visible and near-infrared wavelengths. We expect that the combination of semiconductor metasurfaces with embedded LDE QD emitters will facilitate unexplored multiple quantum emitter phenomena with the potential for novel quantum sensing and communication technologies.

Methods:

Epitaxial Growth: The sample described in this study is grown using molecular beam epitaxy (MBE) on a semi-insulating GaAs (100) substrate (VA1166). The native oxide on the substrate is first thermally desorbed in-situ at 630°C for 10 min. The growth of the epilayers is then initiated at a substrate temperature of 600°C. The structure mainly consists of a 300nm GaAs buffer, followed by a 500nm $Al_{0.75}Ga_{0.25}As$ etch-stop layer and a 140nm thick $Al_{0.4}Ga_{0.6}As$ layer. The latter layer is embedded with LDE GaAs QDs (in the middle – at 70nm) and is protected on both top (from air) and bottom (from the etch stop layer) sides with 5 nm GaAs layers (see SI). For the QD layer, the growth process is paused in the middle of the $Al_{0.4}Ga_{0.6}As$ barrier layer and the substrate temperature is increased to 620°C under an arsenic soak. The excess arsenic on the surface is removed by annealing the substrate at this temperature for 40 seconds without any arsenic supply. Next, only aluminum is introduced to form droplets with a nominal thickness of 0.6ML. The arsenic supply is now opened, and the droplets are annealed in a low-arsenic environment for 300 seconds to promote etching of nanovoids. To form QDs, GaAs is deposited using migration-enhanced epitaxy (MEE) to ensure large diffusion lengths and preferred nucleation inside the nanovoids. This consists of alternate deposition of Ga (0.5 s) and As (10 s) to get a total GaAs QD thickness of 1.75nm (24 loops). The QDs are finally annealed for 300 s before going back to growing the rest of the $Al_{0.4}Ga_{0.6}As$ membrane layer. The Ga and Al growth rates are 0.52 ML/s and 0.34 ML/s respectively for the QD layer. The As:Ga beam equivalent pressure ratio was maintained at 15 for most of the growth and reduced to ~7.5 for a low-arsenic environment. The substrate temperature is measured using a pyrometer. The growth rates are calibrated on a GaAs substrate using reflection high-energy electron diffraction (RHEED).

Fabrication: To define the metasurfaces on the wafer, PMMA 495/950 A2 dual-layered e-beam resist was coated (3000 rpm for 30 seconds) and baked at 180 °C for 1 minute, 30 seconds. The metasurfaces were patterned using the e-beam lithography process (600 μC/cm^2, 100 kV) and developed with MIBK/IPA for 60 seconds. The samples were then dry-etched by the reactive ion etching (RIE) process in a mixture of BCl_3, Cl_2, Ar, and N_2 gases (10, 10, 10, and 3.5 cm^3/min, respectively). After defining the AlGaAs metasurface, the remaining e-beam resist from the metasurface is removed with Remover PG at 75 °C for 20 minutes. The sample is then flip-chip-bonded onto sapphire substrates using epoxy (353ND, EPO-TEK). The GaAs wafer under the metasurface was removed using mechanical lapping and wet-etching processes. Finally, the etch stop layer is removed and only the metasurface remains on the sapphire substrate.

Photoluminescence and $g^2(t)$ Measurement setup: The fabricated samples containing QDs integrated into metasurfaces and into the $Al_{0.4}Ga_{0.6}As$ slab were characterized at *T* = 15+/-5 K using an optical cryostat. A wide-field microscopy configuration and a CCD camera were used to locate QDs within the sample. Then, individual QDs were illuminated in a confocal microscopy configuration using a tightly focused beam from a fiber-coupled 515 nm laser diode running below the lasing threshold. Photoluminescence from individual QDs was collected using a 50X microscope objective (NA = 0.42) and analyzed with a 1200 g/mm grating spectrometer. Two long-pass filers were used to block the excitation beam light from the laser. The same optical setup was used for the optical excitation power dependence experiments (Fig. 4a) and for $g^2(t)$ – correlation function measurements. Two angle-tunable edge filters (short-pass and long-pass) were added to setup for these measurements to isolate emission due to the main optical transition in the QD. $g^2(t) = \frac{\langle n_1(t) n_2(t) \rangle}{\langle n_1(t) \rangle \langle n_2(t) \rangle}$, was estimated by counting the number of photons in each of the two ($n_{1,2}(t)$) super-conducting nanowire broadband detectors as a function of time t.

Transmission measurement Setup: The transmission spectra through the metasurface were measured using a white light (Tungsten Halogen lamp) source and visible spectrometer (Ocean Optics, Jazz) and two 50mm Plano-convex lens above and below the metasurface. The spectra measured through the metasurface was normalized to the transmission through an adjacent region on the sample without the metasurface, containing only the sapphire substrate. The dark counts on the spectrometer were subtracted out from both (metasurface and background) spectra prior to normalization.

Acknowledgement:

SNL is managed and operated by NTESS under DOE NNSA contract DE-NA0003525. This work was supported by the US Department of Energy (DOE), Office of Basic Energy Sciences, Division of Materials Sciences and Engineering and performed, in part, at the Center for Integrated Nanotechnologies, an Office of Science User Facility operated for the US DOE Office of Science.